Abstract—Survey standardization procedures can reduce the variability in trawl catch efficiency thus producing more precise estimates of biomass. One such procedure, towing with equal amounts of trawl warp on both sides of the net, was experimentally investigated for its importance in determining optimal trawl geometry and for evaluating the effectiveness of the recent National Oceanic and Atmospheric Administration (NOAA) national protocol on accurate measurement of trawl warps. This recent standard for measuring warp length requires that the difference between warp lengths can be no more than 4% of the distance between the otter doors measured along the bridles and footrope. Trawl performance data from repetitive towing with warp differentials of 0, 3, 5, 7, 9, 11, and 20 m were analyzed for their effect on three determinants of flatfish catch efficiency: footrope distance off-bottom, bridle length in contact with the bottom, and area swept by the net. Our results indicated that the distortion of the trawl caused by asymmetry in trawl warp length could have a negative influence on flatfish catch efficiency. At a difference of 7 m in warp length, the NOAA 4% threshold value for the 83-112 Eastern survey trawl used in our study, we found no effect on the acoustic-based measures of door spread, wing spread, and headrope height off-bottom. However, the sensitivity of the trawl to 7 m of warp offset could be seen as footrope distances off-bottom increased slightly (particularly in the center region of the net where flatfish escapement is highest), and as the width of the bridle path responsible for flatfish herding, together with the effective net width, was reduced. For this survey trawl, a NOAA threshold value of 4% should be considered a maximum. A more conservative value (less than 4%) would likely reduce potential bias in estimates of relative abundance caused by large differences in warp length approaching 7 m.

Manuscript submitted 20 October 2004 to the Scientific Editor's Office.

Manuscript approved for publication 6 June 2005 by the Scientific Editor.

Fish. Bull. 104:21–34 (2006).

Variation in trawl geometry due to unequal warp length

Kenneth L. Weinberg

David A. Somerton

National Marine Fisheries Service
Alaska Fisheries Science Center
7600 Sand Point Way N.E.
Seattle, Washington 98115-0070

E-mail address (for K. L. Weinberg): ken.weinberg@noaa.gov

Standardization of trawl survey procedures can reduce the variability in abundance indices between samples, survey vessels, and over time by reducing the variability in trawl catch efficiency. Such standardization was the focus of the recently developed U.S. National Oceanic and Atmospheric Administration (NOAA) protocols for the operation of its groundfish bottom trawl surveys (Stauffer, 2004). The first of these protocols concerns the measurement of towing cables or warps. For vessels towing with two warps, the NOAA protocols specify that the difference in length between port and starboard warps may not exceed 4% of the wire length between otter doors measured along the bridles and footrope. The need for adopting such a critical value was considered essential because of the belief that unequal warp lengths—from inaccurate measurement or subsequent stretching—would lead to distortion of trawl geometry and a change in catch efficiency, particularly for operations that use trawl winches with the brakes set or locked. The adopted value, however, was chosen somewhat arbitrarily because experimental data showing the dependency of trawl geometry or fishing performance on warp symmetry was lacking for any of the bottom trawl surveys subject to the protocols.

In this study, we examine the effect of unequal warp lengths on the geometry of the 83-112 Eastern trawl which is used by the Alaska Fisheries Science Center (AFSC) to conduct the annual eastern Bering Sea shelf survey. Although we monitor a full suite of trawl dimensions, such as door spread, wing spread, and headrope height that are typically measured on trawl surveys, our attention was primarily focused on the distance between the footrope and lower bridles with the sea floor. Prior studies with this trawl have demonstrated that escapement under the footrope (Somerton and Otto, 1999; Munro and Somerton, 2002; Weinberg et al., 2004) and herding by the bridles (Somerton and Munro, 2001) are the most important determinants of catch efficiency for flatfishes and other benthic species. Although we understand that catch efficiency depends on animal behavior as well as trawl geometry, a goal of our study was to assess whether the 4% critical value is appropriate to prevent an appreciable degradation of catch efficiency due to warp asymmetry, the result of unequal trawl warp lengths.

Materials and methods

Experimental design

The experiment was conducted during 14–17 September 2003 along the Alaska Peninsula in Bristol Bay approximately 85 km NE of Amak Island (55°58′N, 162°55′W) on smooth, relatively level bottom at a depth of 82 m. Trawling was performed with the chartered 38-m stern trawler FV *Vesteraalen*. The *Vesteraalen* is powered by a single 1725-hp engine and is equipped with split Rapp Hydema (Rapp Hydema AS, Bodø, Norway) trawl winches carrying 2.5 cm (1″) diameter, compacted, solid-core trawl warp.

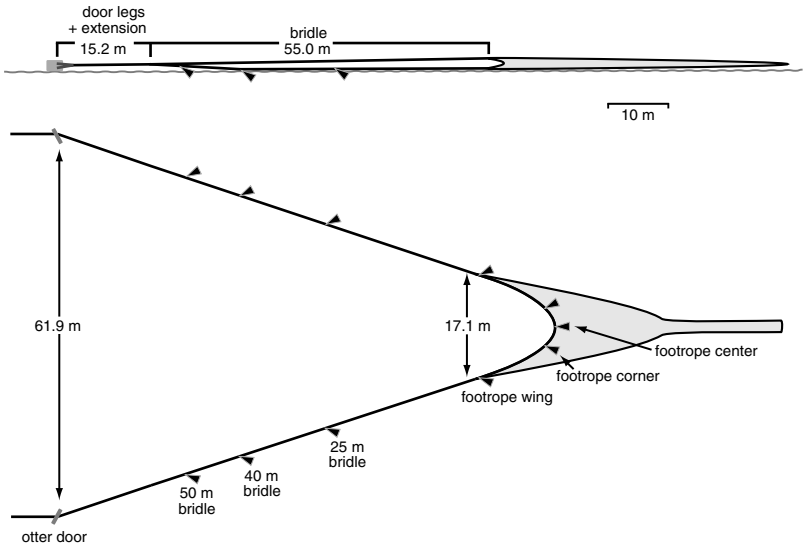

Figure 1

Schematic diagram of the 83-112 Eastern survey trawl and rigging shown from the side (upper panel) and from above (lower panel). The experimentally determined mean door spread and wing spread dimensions shown apply when towing at a depth of 82 m with 274 m of trawl warp on each side. Bottom contact sensor units, shown as oversized triangles along the bridles and footrope, are labeled by position as discussed in the text.

The 83-112 Eastern is a low-rise, 2-seam, flatfish trawl designed for use on smooth, soft bottom. The nylon net is constructed of 10.1-cm stretch mesh in the wing and body, 8.9 cm in the intermediate, and double 8.9-cm mesh lined with a 3.1-cm mesh in the codend. It is towed behind a pair of 1.8×2.7 m steel "V" doors, weighing approximately 816 kg apiece, which are attached to the net by two 3-m-long door legs (consisting of 1.6-cm long-link chain); a 12.2-m-long door leg extension (consisting of 1.9-cm diameter stranded wire); and a pair of 55-m-long, bridles (consisting of 1.6-cm diameter bare stranded wire) on each side of the net (Fig. 1). The 25.5-m-long (83 ft) headrope has 41 evenly spaced, 20.3-cm diameter floats that provide 116.4 kg of total lift. The 34.1-m-long (112 ft), 5.2-cm diameter footrope is constructed of 1.6-cm diameter stranded-wire rope protected by a single wrap of both 1.3-cm diameter polypropylene line and split rubber hose. The footrope is weighted with 51.8 m of chain (0.8-cm proof-coil) attached at every tenth link, forming 168 loops to which the netting is hung. An additional 0.6-m-long, 1.3-cm long-link chain extension connects each lower bridle to the trawl wing tips to help keep the footrope close to the bottom. Because the wire length between otter doors measured along the bridles and footrope is 175.6 m, the critical value for differential warp length for this trawl established by the NOAA 4% rule is 7 m.

Prior to the experiment, the warp length to be used was measured to the nearest 0.1 m with a calibrated, in-line wire counter (Olympic 750-N, Vashon, WA). A zero reference point was painted on each trawl warp, as determined by first setting the wire counter to zero with the trawl door just beneath the water surface and then measuring out 274 m (150 fm), the survey standard warp length for a fishing depth of 82 m. To verify this benchmark measurement, the process was repeated and all replicate measurements were found to be within 0.3 m, which is less than the 1 m specified by the NOAA trawl survey protocols for replicate measurements. Subsequent reference marks, measured by tape, were then placed along each warp at 3, 5, 7, 9, 11, and 20 m from the zero mark.

The experiment consisted of examining the effect of seven differences in warp length, henceforth referred to as "offsets," where one warp was positioned at values of 0, 3, 5, 7, 9, 11, or 20 m longer. An experimental set consisted of all seven offsets, chosen in random order. A treatment consisted of towing the trawl, with the winch brakes locked, at the specified offset for 5 minutes at 3 knots while maintaining a constant vessel heading. Treatments were preceded by a 2-min equalization period at the specified offset. A haul consisted of two treatment sets: one with a port offset and the other with a starboard offset—the order having been chosen randomly for each haul. To minimize the effect of bottom currents on trawl symmetry, hauls were made in pairs along the axis of the dominant current direction, either with or against the current—again, the order having been chosen randomly. This direction was determined by deploying a current meter (Nobska MAVS-3, Woods Hole, MA) 3 m above the bottom for one day

prior to the start of the experiment. Hauls were made with the trawl codend open to eliminate any catch effects on trawl geometry.

Several measures of trawl geometry and performance were taken during each treatment. The distance between the doors (door spread), the wing tips (wing spread), and the center of the headrope to the sea floor were measured acoustically with Scanmar sensors (Scanmar, Asgardstrand, Norway) to 0.1 m at 4-s intervals. Water flow, both perpendicular and tangential to the headrope, was measured to 0.1 knot at 24-s intervals with a Scanmar trawl speed sensor placed at the center of the headrope. Vessel position was measured with satellite navigation at 2-s intervals. Bridle tension was measured in kilograms at 2-s intervals using in-line tension recorders (Billings Ind. TR-999, N. Falmouth, MA) attached behind the door legs. Bottom current velocity in cm/s and direction data were recorded at 10-s intervals.

Footrope off-bottom distance was measured at five positions simultaneously by placing bottom contact sensors (BCS) at the center of the footrope, at the corners located 3 m to either side of the center, and on each wing 1 m behind the wing tip (Fig. 1). These sensors are self-contained units consisting of a tilt meter, which measured angle to the nearest half degree at 0.5 s elapsed time intervals, and a data logger housed in a watertight stainless steel container that fits inside a steel sled (Somerton and Weinberg, 2001). One side of this sled clips into a clamp on the footrope, which allows that end of the sled to pivot freely about the footrope while the other end drags along the bottom (Fig. 2). In this way, changes in the distance of the footrope from the bottom produced changes in the recorded tilt angle. Conversion from tilt angle to distance off-bottom was accomplished by applying a calibration function derived for each BCS unit by fitting a quadratic function to data from an experiment in which angles associated with known distances from a hard surface were measured. The BCS unit extended 44 cm behind the footrope and weighed (BCS, sled, and footrope clamp) 8.9 kg in seawater. The clamp extended beneath the footrope by 2 cm and, depending on the extent of penetration into the sediment, could raise the footrope off the bottom (Fig. 2). Because the degree of penetration is unknown, no adjustments to our calibration functions were made.

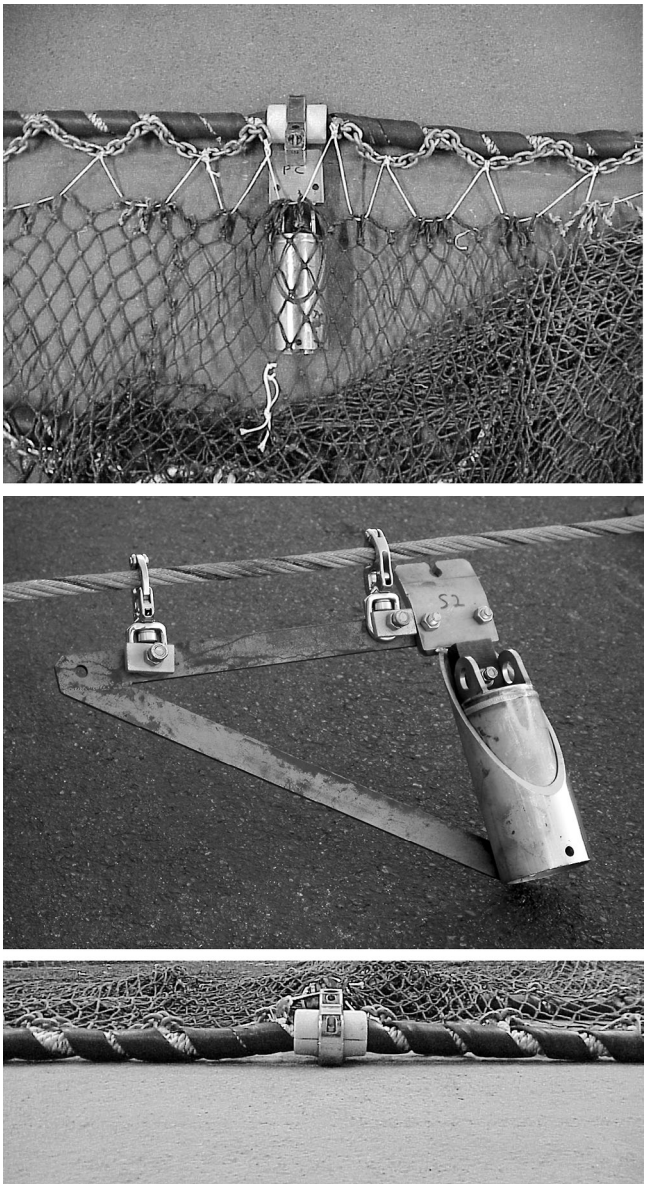

Figure 2

Bottom contact sensors shown mounted to the footrope (upper) and bridle (middle). The footrope shown in the "on-bottom" position without lateral tension and on a hard surface is elevated 2 cm by the footrope clamp (lower).

Bridle off-bottom distance was measured at six positions simultaneously by placing BCS units on the lower bridle at distances of 25, 40, and 50 m forward of the wing tip on both sides of the trawl (Fig. 1). However, the BCS units used on the bridles differed from those used on the footrope. These units were mounted on a triangular frame designed to hold the BCS perpendicular to the bridle (Fig. 2; Somerton, 2003). The triangular frame measured 49 cm in its longest dimension and was held in place by a cable stop that also extended beneath the bridle by about 2 cm. The weight of a bridle BCS unit and frame was 8.7 kg in seawater.

Data analyses

Three tilt angle measurements from each BCS unit were averaged for each 1.5-s interval, converted to distance off-bottom by applying the calibration function determined for that unit, and then the off-bottom distances

were averaged for each experimental treatment on each haul. Mean off-bottom distances for each bridle and footrope position, except the footrope center, were grouped by offset distance (i.e., long side vs. short side of an experimental treatment) where, for example, the distance measurements from the 25-m position on the starboard bridle collected on a starboard treatment (long side) was grouped with the measurements from the 25-m position on the port bridle during a port treatment. Under these groupings, we assumed equality and subsequently refer to the offsets by whether they were on the long or short side (e.g., long 5 m) rather than whether they were on the port or starboard side (e.g., port 5 m).

To allow interpolation between the experimental offsets, cubic spline models (Venables and Ripley, 1994) were fitted to door spread, wing spread, headrope height, and the off-bottom distances for each bridle and footrope position as a function of offset. Bootstrapped empirical 95% confidence intervals (CI; Efron and Tibshirani, 1993) were estimated for all measured categories as described in the following example for off-bottom distance as follows: 1) assuming that mean off-bottom distances within a set were correlated because of local environmental conditions, we chose 1000 bootstrap replicates by sampling entire sets of measurements with replacement; 2) we fitted a cubic spline, weighted by the inverse of the variance, to each bootstrap sample, and then predicted the mean off-bottom distance for each 1 m of offset; and 3) we ranked the predicted values, then chose the 25th highest and lowest values as the CI bounds. Similarly, we estimated the empirical 95% CIs about the mean off-bottom distance at zero offset in the same manner except that only zero offset treatments were considered.

Modeling trawl shape

To help visualize the distortion of the trawl that occurs in response to offset, we created three views of the trawl: 1) the shape of the lower bridle when viewed laterally, 2) the shape of the headrope when viewed from above, and 3) the shape of the footrope when viewed from in front of the trawl. In addition, we calculated the area swept by the bridles (herding area) and the effective net width (i.e., the greatest lateral dimension of the net).

Bridle shape and herding area

The shape of the lower bridle, when viewed laterally (i.e., off-bottom distance as a function of position along the bridles), was approximated by linear interpolation between the mean off-bottom distances measured at the wing, and the 25-, 40-, and 50-m bridle positions. Such shape functions were calculated for both the long side and the short side of the trawl at each offset increment.

The herding area can be considered as a function of the bridle contact length, that is, the length of the bridle that is sufficiently close to the bottom to elicit a herding response (Somerton and Munro, 2001) and the angle-of-attack between the bridle and the direction of travel (α). For flatfish, the vertical distance of the bridle from the sea floor at which a herding response is initiated (reaction height) will vary with species, size, viewing conditions, arousal state, and other variables, but for illustrative purposes, we considered a reaction height of 1 cm where video observations indicated that this value is appropriate for a small flatfish, initially at rest and unaware of the approaching bridle (Somerton, unpubl. data). Thus the value of the bridle contact length was determined as the distance between the wing tip and the point along the bridle at which the interpolated value of off-bottom distance reached the reaction height. The angle-of-attack, α, was not measured during the experiment; however, when the trawl is symmetric, α can be modeled as

$$\alpha = \mathrm{Sin}^{-1}\left(0.5(D-W)/B\right),$$

where D = the distance between doors;
W = the distance between wing tips; and
B = the distance between the wing tip and the door.

It is not clear, however, how α will differ between the long and short side of the trawl when warp offsets occur. For illustrative purposes, we assumed that α is symmetrical and remains constant during all experimental values of warp offset. Thus, for each side of the trawl and for each offset, a value of bridle contact length and α were first calculated as above, then the width of the herding area on each side of the trawl was computed as the bridle contact length times sin (α) and the two areas were summed together.

Headrope shape and effective net width

The curved shape of the headrope when viewed from above can be approximated as a quadratic (parabolic) function when the warps are equal in length and there are no external forces to distort the symmetry of the net (Fridman, 1969). If the shape remains parabolic as the warp offset is increased, then the headrope shape can be uniquely determined with three geometric measurements: 1) the length of the headrope; 2) the distance between wing tips; and 3) the tangent to the headrope at its center. The first quantity was measured at the start of the experiment. The second quantity was measured acoustically on all hauls, and then averaged by treatment. The third quantity was calculated as the quotient of the tangential water velocity (U) divided by the perpendicular velocity (V) measured by the headrope speed sensor (i.e., U/V). With these quantities, the headrope shape was determined as described in Appendix A.

Although the shape of the headrope determined by this method is assumed to be parabolic, the headrope becomes increasingly asymmetric about the direction of travel as the degree of warp offset increases because the wing tip on the short side of the net precedes that on the long side. When this distortion occurs, the mea-

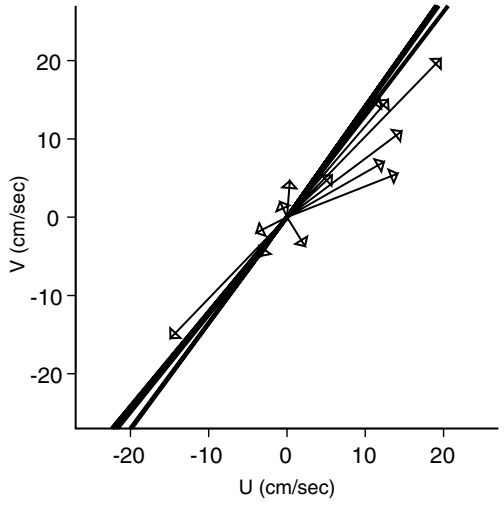

Figure 3

Current velocity vectors during each of the 13 experimental tows are shown with arrows. Vessel direction during these tows is shown with the dark lines. The axes, labeled U and V, indicate the latitudinal and meriodonial components of the velocity vectors in cm/s.

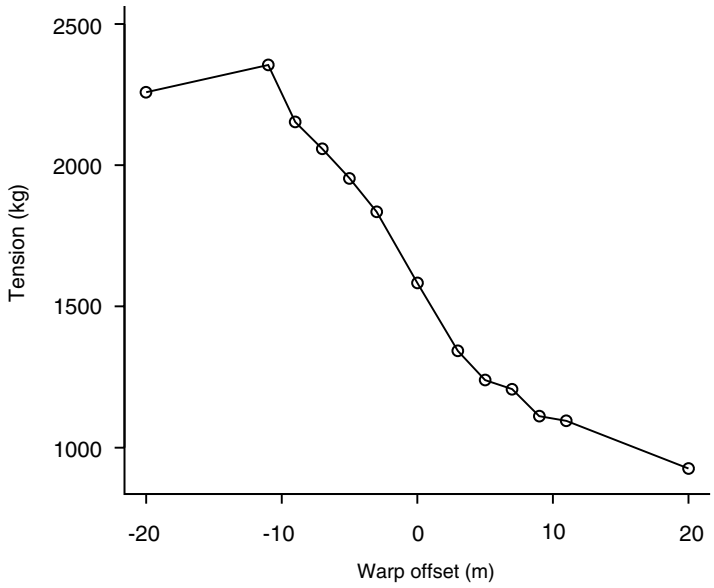

Figure 4

Mean tension (in kilograms) measured on both port and starboard door legs is shown plotted as a function of warp offset in meters. Note that on the side with the shorter warp (negative offset), tension is higher than when the warps are equal and that on the side with the longer warp, the tension is lower.

sured distance between wing tips becomes increasingly greater than the effective net width (i.e., the distance from wing tip to wing tip projected on a plane perpendicular to the direction of travel). The method used to estimate effective net width was based on headrope geometry and is described in Appendix A.

Footrope shape viewed from the net mouth

Because of footrope geometry, the importance of footrope bottom contact to overall net efficiency varies along the length of the footrope. This feature is true not only because escapement probability likely changes with the angle of the footrope in relation to the direction of travel but also because the proportion of the net width spanned by a unit length of footrope varies. To help visualize the latter effect better, we projected the off-bottom distances from their positions along the footrope onto a plane that was perpendicular to the direction of travel and spanned by the effective net width, using the footrope shape model determined for each offset increment described in Appendix A.

Results

Twelve successful tows consisting of 24 sets of treatments were completed during the experiment. Bottom current velocities ranged from about 5 cm/s to about 30 cm/s and current direction was approximately parallel to the trawl towing direction (Fig. 3); consequently the mean current velocity perpendicular to the towing direction was quite small (1.8 cm/s).

Bridle tension and geometry

For the single haul in which both tension meters worked successfully, the bridle tension, combined over both sides, did not change significantly when regressed on the warp offset (df=11, P=0.69). This result indicates that any distortion of the trawl due to the offset treatments was not sufficient to appreciably affect the combined tension and, therefore, the hydrodynamic and frictional drag of the net and the bridles. However, changing the relative length of the warps resulted in a progressive transfer of the tension to the shorter warp (Fig. 4). For example, based on the average combined bridle tension (3248 kg), when the difference in warp lengths was 11 m, the shorter warp carried 72% of the total net and bridle drag.

Headrope speed through the water

The velocity component perpendicular to the headrope (U) decreased with increasing warp offset, whereas the absolute value of the velocity tangential (velocities from the port side of the sensor are opposite in sign to velocities from the starboard side) to the headrope (V) at its

center increased (Fig. 5). We interpret this as indication that the speed sensor at the headrope was rotated in relation to the direction of travel as the warp offset was increased. Calculating the angle between the perpendicular at the center of the headrope and the direction of travel as $\tan^{-1}(U/V)$, the angle increased from 11° at 3 m offset to 61° at 20 m offset. Although the absolute value of the tangential velocity was measured at values >0 at zero offset, the tangential velocity was not significantly different than zero (t-test, P=0.71). This result indicates that the alignment of the experimental tows in relation to the prevailing current was sufficient to reduce the cross current to negligible levels.

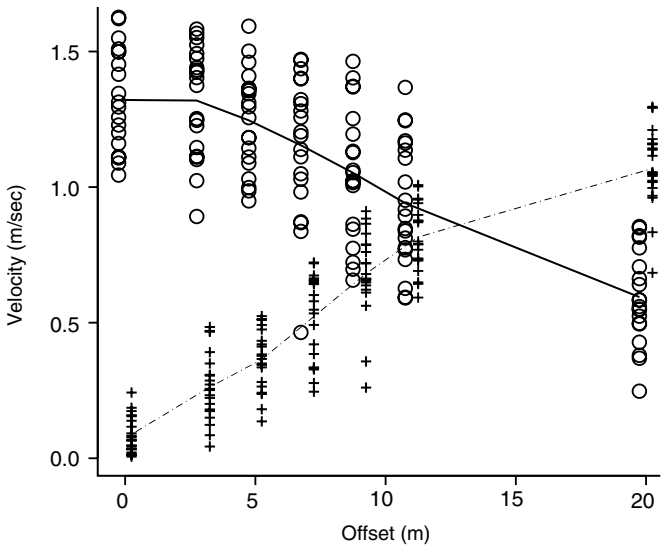

Figure 5

Current velocity (in m/sec) measured at the center of the headrope for each tow is shown separated into the component perpendicular to the headrope (O) and the component tangential to the headrope (+). The solid and dashed lines connect the means at each offset increment. Note, for clarity, that the offsets are incremented by plus or minus 0.1 m for the tangential and perpendicular components.

Net and door measurements

At zero offset, the mean door spread obtained was 61.9 m. The mean wing spread was 17.1 m, and the mean headrope height was 2.0 m. Differences in the means of all three quantities were not apparent at lower offsets, however headrope height and wing spread were more sensitive to changes in large offsets because both were significantly (P<0.05) greater than the zero offset means when offset was increased to 11 m, whereas door spread did not differ significantly until the offset was approximately 14 m (Fig. 6).

Bridle and footrope distance off-bottom by position

Bridle and footrope off-bottom distance varied considerably with position, not only with respect to the mean value but also with respect to the sensitivity of the mean to changes in offset. At zero offset, the mean off-bottom distance of the bridle declined from 12.3 cm at 50 m from the wing tips, to 3.2 cm at 40 m and 2.0 cm at 25 m (Fig. 7). Mean off-bottom distance remained small along the footrope, varying from 1.7 cm at 1 m behind the wing tip to 2.5 cm at the corner and 1.9 cm at the center.

The mean response to changes in offset varied greatly by position. Along the bridles, the most sensitive location was at 50 m, where off-bottom distance increased on the short side and decreased on the long side with increasing offset (Fig. 7). At 40 m, a similar pattern was repeated, but for most offsets on the long side, the off-bottom distance was near the minimum recorded, indicating that the bridle was resting on the bottom. At 25 m, the bridle was nearly always in contact with the bottom and off-bottom distance was insensitive to variations in warp offset. Along the footrope, the most sensitive position was the corner where off-bottom distance increased greatly with offset, particularly with positive offsets due to the relaxation in warp tension. At the center of the footrope, off-bottom distance was also sensitive to warp offset, responding almost identically on the long and short sides. At 1 m behind the wing tip, sensitivity to warp offset was quite low and the off-bottom distance indicated that the footrope was in contact with the bottom except for large offsets on the long side.

An alternate method of assessing the sensitivity of geometry of the 83-112 Eastern trawl to changes in offset is to determine if the mean off-bottom distance at 7 m, the maximum offset allowed under the NOAA protocols for the 83-112 Eastern trawl, differs statistically from the mean off-bottom distance at zero offset. Based on the bootstrapped confidence intervals (Fig. 7), off-bottom distance is significantly different from what it is at zero offset at the 50-m and 40-m bridle positions and at the center and corner footrope positions but is not significantly different at the wing and the 25-m bridle position.

Bridle shape and herding area

To understand better how the change in tension that accompanies offsets in warp leads to changes in bridle shape, we show the mean off-bottom distances plotted against the BCS positions on the wing and bridles for both the short side and long side of the trawl. From this perspective it is clear that as the tension is increased, off-bottom distance increases on the forward part of the bridle. Likewise, as the tension is reduced, the off-bottom distance decreases (Fig. 8). For flatfish, the effect of these changes in off-bottom distance is a change in the area subjected to herding stimuli. For the case where the reaction height is 1 cm, the bridle contact length is determined by the intersection of the line depicting

the reaction height with the lines depicting the bridle shape at each offset (Fig. 8). The change in these lengths on the short and long sides of the trawl is asymmetric with changes in warp offset (Fig 9). For the long side, bridle contact length increases linearly with positive offset. However, for the short side, bridle contact length decreases nonlinearly with warp offset—the greatest changes occurring with small offsets. This difference likely leads to a change in the total width of the herding area with changes in warp offset. If, for example, it is assumed that the angle-of-attack (α) is the same for the long and short sides of the trawl, then the width of the herded area declines to a minimum at about 8 m offset, at which the herded area is reduced by 10.3% compared to that at zero offset.

Headrope shape and effective net width

With increasing difference in warp length, the model we used to describe headrope shape predicts three distinct changes in shape. First, the headrope is distorted so that the wing tip on the short side of the trawl precedes that on the long side in the direction of travel (Fig. 10). The difference in the forward position of the wing tips, however, is much less than the warp offset. For example, an 11-m difference in warp length resulted in an offset in the position of the wing tips of only 2–3 m. This difference occurs because the increased tension on the short warp changes the catenary in both the bridles and the warps (i.e., both become effectively longer as the sag is reduced). Second, the headrope is distorted so that its center is increasingly displaced away from the midpoint between wings and toward the short side of the trawl. When this displacement occurs, the perpendicular at the center of the headrope is no longer aligned with the direction of travel. Third, the headrope is distorted so that the effective width of the net (i.e., the wing spread projected to the line perpendicular to the towing direction) becomes increasingly shorter than the distance measured by the acoustic net sensors. The difference between the effective and the measured net width is negligible for offsets up to 7 m but rapidly increases at greater offsets (Fig. 11).

Footrope shape viewed from in front of the net

The distance of the footrope off-bottom, when viewed from a position in front of the net, increases with increasing offset; however, the location of the maximum off-bottom distance in relation to the midpoint between wings, shifts slightly with increasing offset (Fig. 12). With offsets of 9 m or less, the position of maximum off-bottom distance is at the corner of the footrope on the long side of the trawl. However, with increasing offset, the shift in the position of the footrope corner changes because of the rotation of the trawl in relation to the direction of travel; and at a 20-m offset the footrope corner on the long side of the trawl is positioned, when viewed on a plane perpendicular to the direction of travel, almost exactly midway between the wing tips.

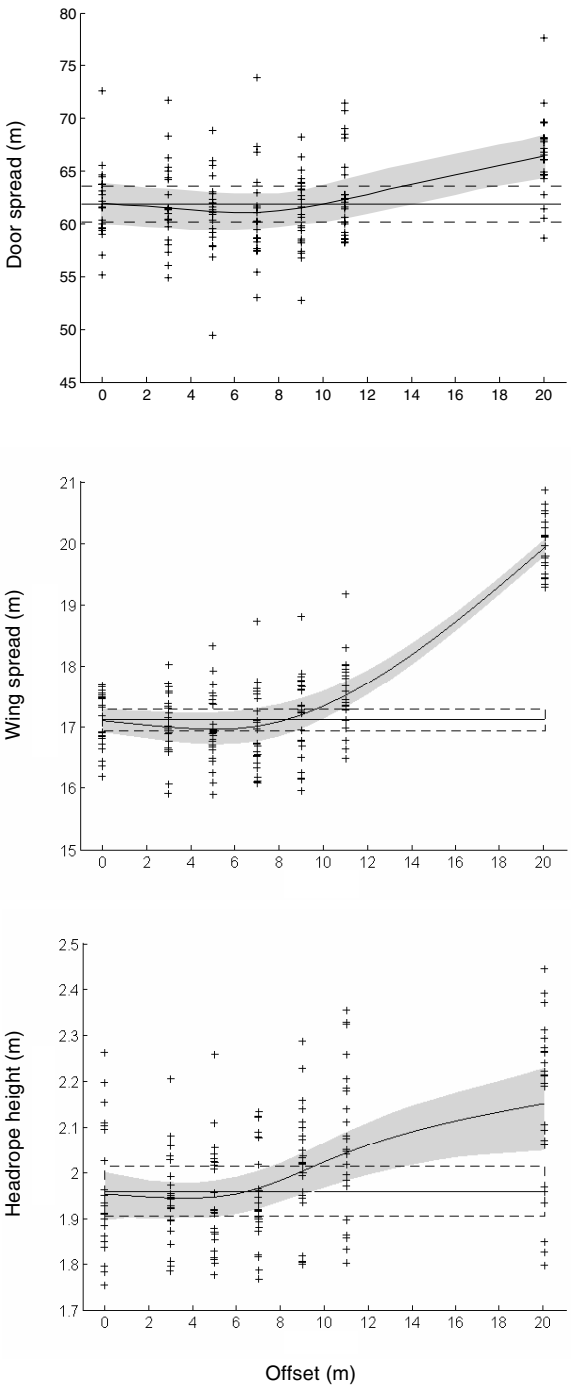

Figure 6

Mean door spread, wing spread, and headrope height are shown (+) plotted against offset increment. The means for all values of offset increment were fitted with a cubic spline function (solid curve). Bootstrapped 95% confidence bounds are shown with shading. Also shown are the mean door spread, wing spread, and headrope height for treatments with zero offset (solid horizontal line) and the corresponding bootstrapped 95% confidence bounds (dashed horizontal lines).

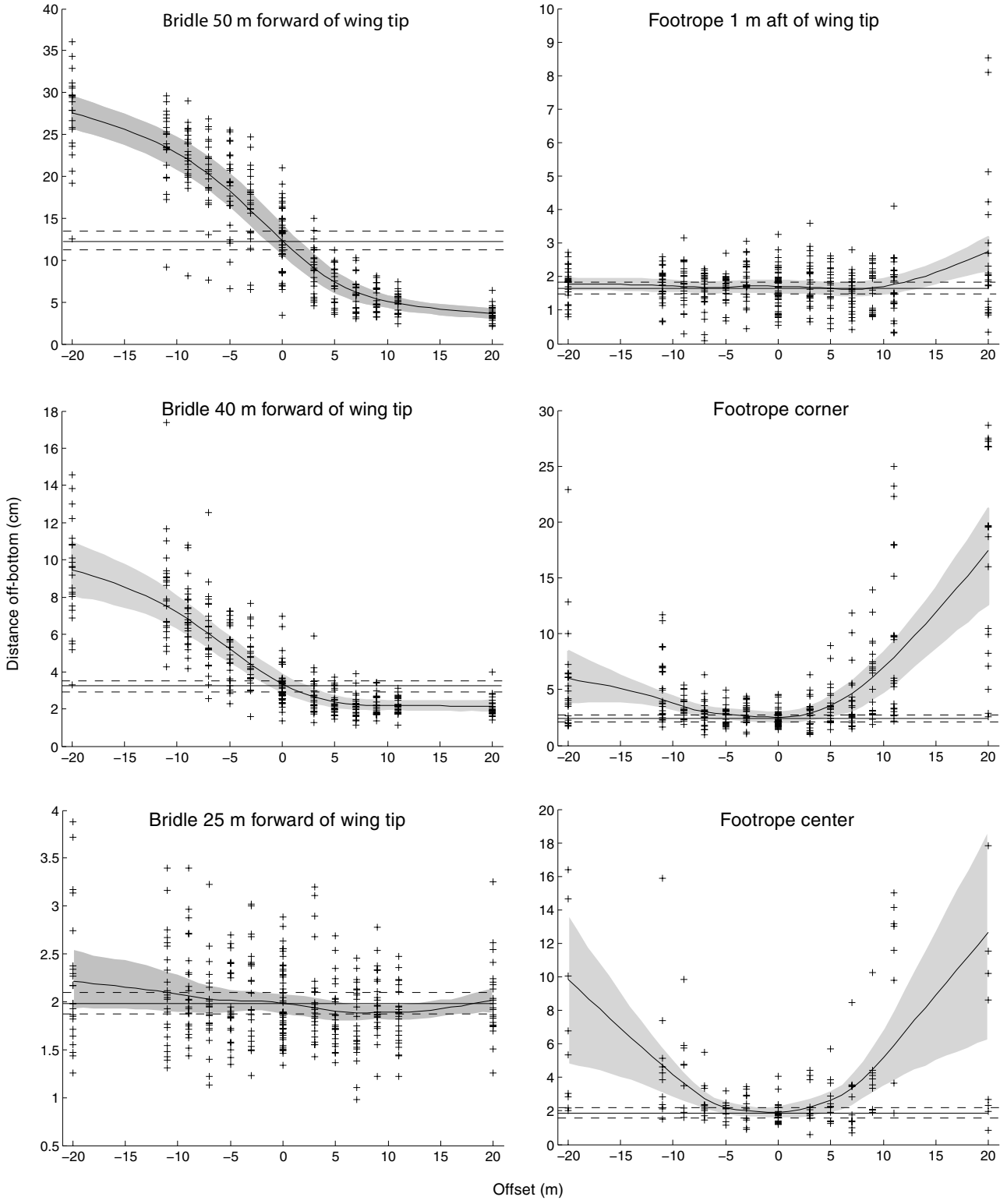

Figure 7

Mean bridle and footrope distance at each bottom contact sensor position is shown (+) plotted against offset increment. The means for all values of offset increment were fitted with a cubic spline function (solid curve). Bootstrapped 95% confidence bounds are shown with shading. Also shown is the mean distance off-bottom for only treatments with zero offset (solid horizontal line) and the bootstrapped 95% confidence bounds (dashed horizontal lines).

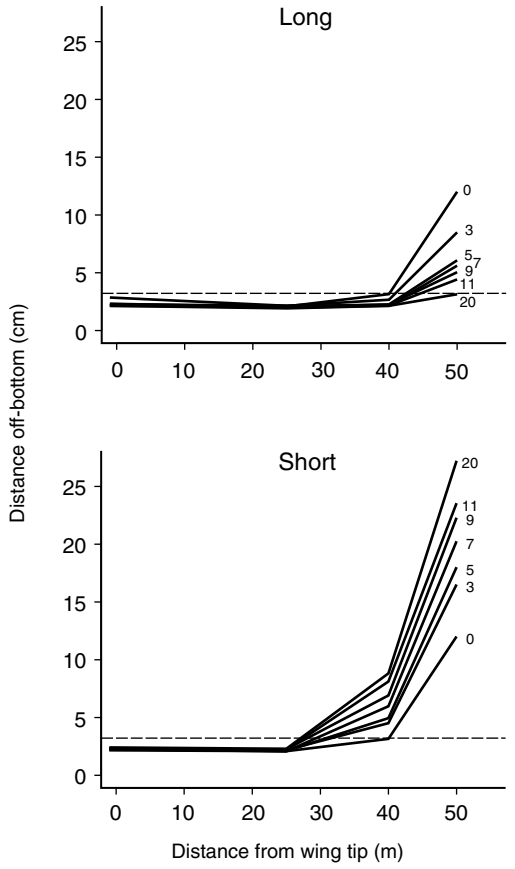

Figure 8

Mean off-bottom distance is shown plotted against the distance measured from the wing tip to the positions of the wing and the three bridle bottom contact sensors. This approximation to the shape of the bridle when viewed laterally is shown for each of the offset increments for both the side with the longer warp and the side with the shorter warp. The dashed line represents the hypothetical reaction height of a fish. The intersection of the dashed line with the solid line for each configuration defines the bridle length that is sufficiently close to the bottom to elicit a herding response.

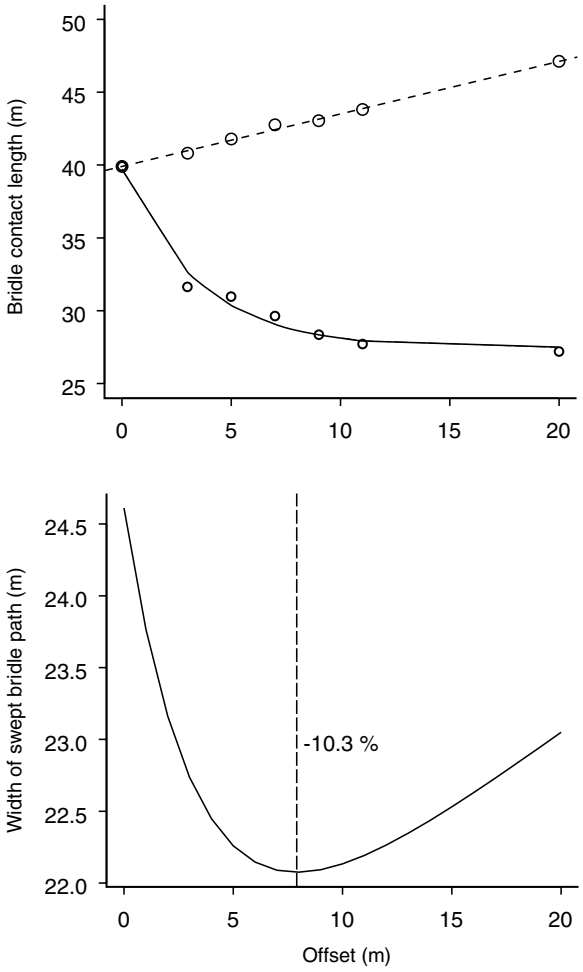

Figure 9

The length of the bridle with the off-bottom distance <1 cm is shown plotted against the offset increment in meters for both the short warp (solid line) and long warp (dashed line) sides of the trawl (upper panel). In both cases the lines are represented using cubic spline smoothing functions. The width of the swept bridle path as a function of warp offset is represented in the lower panel.

Discussion

There are two distinct approaches for judging whether a difference in warp length between the sides of a survey trawl will lead to a significant bias in estimates of relative abundance. In both approaches we focused on the adequacy of the maximum 7-m offset allowed for the 83-112 Eastern trawl under NOAA trawl survey protocols. In the first approach, we simply asked whether, given the sampling effort used in the experiment, any of the measured dimensions at 7-m offset were statistically different from zero offset. In our experiment, none of the three standard measures of trawl geometry (i.e., door spread, wing spread, and headrope height) differed from mean values at zero offset. This finding indicates that either these dimensions are fairly robust to changes in warp offset or that the acoustic measurement of these dimensions was insufficiently precise to detect a difference. Off-bottom distance, however, was significantly different at the two forward positions on the bridles and along the footrope at the center and corner positions.

From the perspective of trawl survey standardization, however, the detectability of changes in geometry is not of primary importance; these changes, however, may produce a significant effect on estimates of relative abundance. Bias in these estimates could result either because the change in trawl geometry leads to an inac-

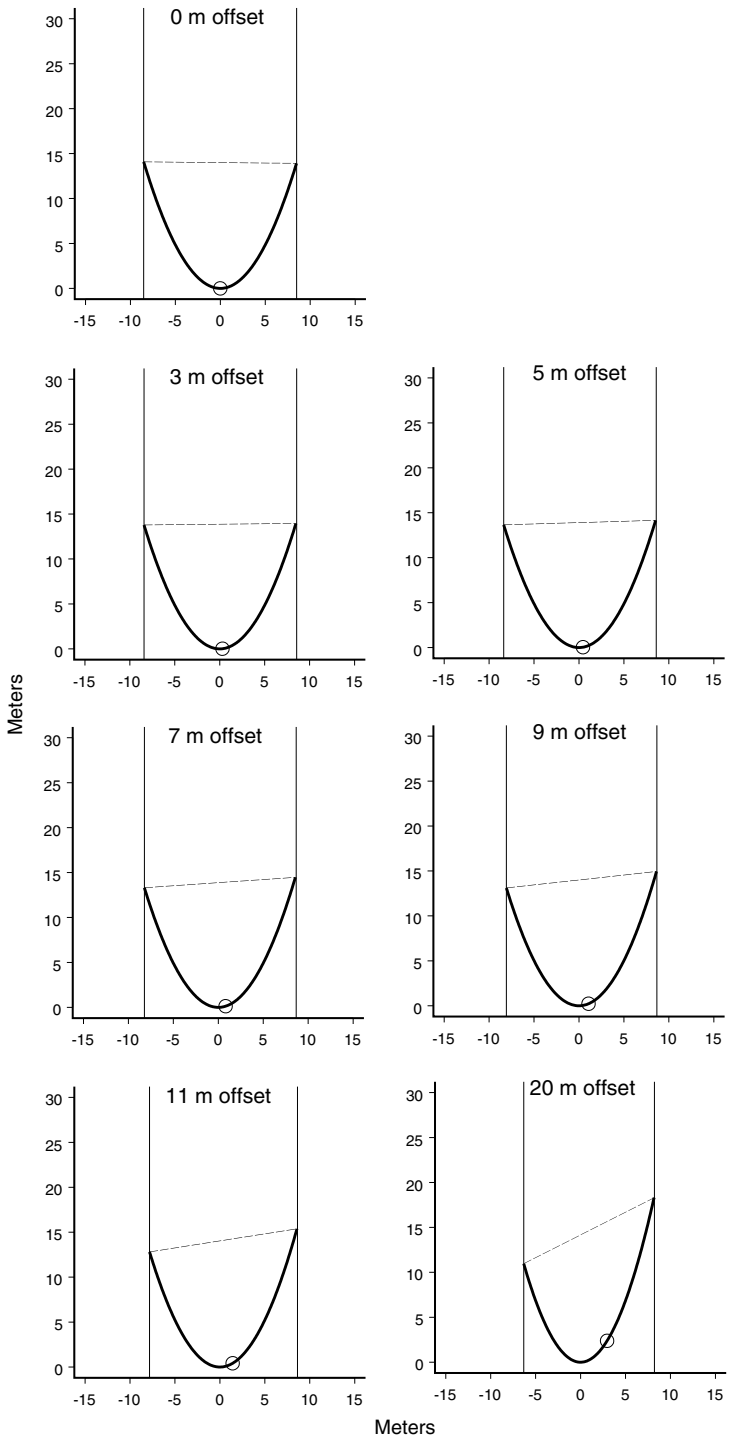

Figure 10

Estimated net shape (curve) and position of headrope center (O) at varying levels of warp offset. The mean distance between wing tips that was acoustically measured during the experimental tows is indicated with a dashed line. The maximum lateral dimensions of the net are indicated with solid vertical lines. The distance between these lines is the effective net width needed for estimating the area swept by the net.

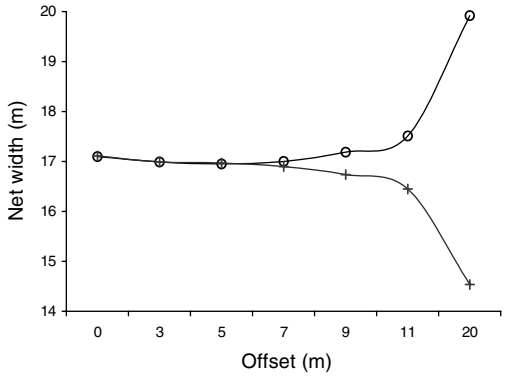

Figure 11

The mean distance between wing tips measured acoustically (O) during the experimental tows (net width) and the calculated effective net width (+) are shown plotted against the offset increment in meters. Note that there is little difference between the two measures of net width until the offset increment is increased to 9 m.

curate measurement of swept area or because it leads to a change in catch efficiency.

Relative abundance indices produced for the eastern Bering Sea shelf survey are based on catch per area swept between the trawl wings. As the net distorts on account of differential warp length, the effective net width will become increasing less than the width that is acoustically measured during the survey. Thus, net width will become increasingly overestimated and relative abundance of fish species therefore will be underestimated. At 7-m offset, however, the measured net width differed from the effective net width by only 0.5%, and therefore this source of error is unlikely to contribute to bias in the swept area estimates. However, the difference between measured and effective net width increases rapidly at greater offsets and could present a problem if a less restrictive threshold value of offset were used.

Catch efficiency of the 83-112 Eastern trawl depends primarily on 1) herding by the bridles, doors, and the mud clouds they create; 2) the escapement under the footrope; and 3) the escapement through the mesh in the body of the net. The relative importance of these three processes, however, will vary for the major species groups that are targeted in the surveys. Gadoids (primarily walleye pollock [*Theragra chalcogramma*] and Pacific cod [*Gadus macrocephalus*] appear to have little or no herding response to the 83-112 Eastern trawl (Somerton, 2004) and rarely pass under the footrope (Somerton, unpubl. data). However, both Pa-

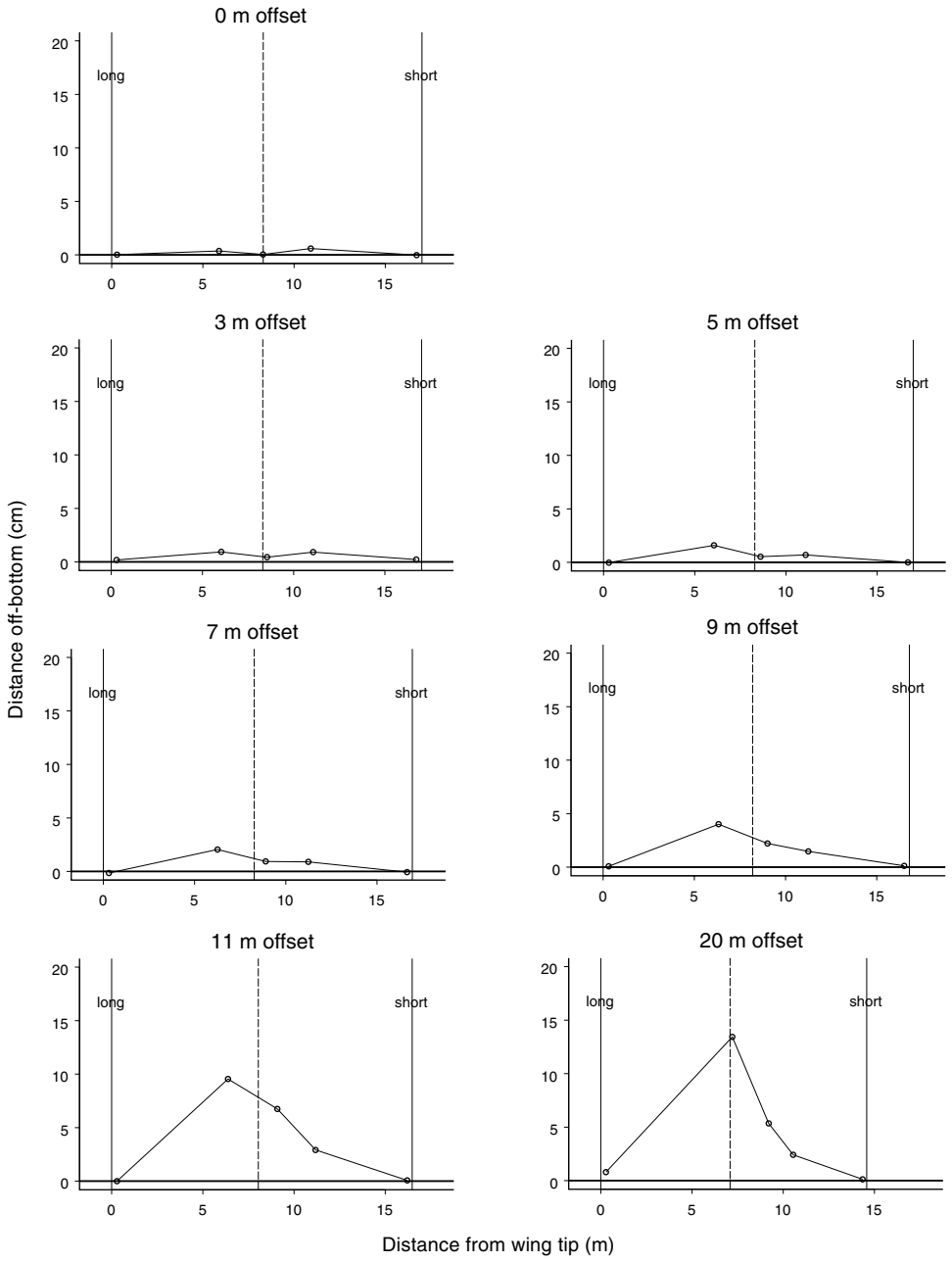

Figure 12

Mean off-bottom distances (in cm) at the five bottom contact sensor positions along the footrope (circles) are shown for each warp offset. The positions are projected onto the wing tip to wing tip plane to depict the footrope as it would appear if one were looking into the net from the direction of travel. The vertical solid lines indicate the positions of the wing tips on the long warp and short warp sides of the trawl. The dashed line indicates the midpoint between wing tips. Note that the projection considers the reduction in effective net width with increasing offset.

cific cod and walleye pollock are found gilled in the body of the net; therefore some mesh escapement may occur, especially if any distortion of the net results in altered water flow through the meshes. Video observations of crabs (snow and Tanner crabs [*Chionoecetes* sp.] and king crabs [*Paralithodes* sp.] show that they also exhibit little or no herding response to the 83-112 Eastern trawl (Weinberg, unpubl. data). However, both

Chionoecetes species (Somerton and Otto, 1999) and red king crab (Weinberg et al., 2004) do escape under the footrope. Flatfishes (including yellowfin sole [*Limanda aspera*], flathead sole [*Hippoglossoides elassodon*], and rock sole [*Lepidopsetta bilineata*] display a strong herding response to the 83-112 Eastern trawl (Somerton and Munro, 2001); as much as 49% of the catch consisted of fish that were herded by the bridles into the net path. Likewise, flatfishes are readily capable of escaping under the footrope and, for species such as yellowfin sole, at least 25% of the largest individuals escape in this manner (Munro and Somerton, 2002). Thus, the capture efficiency of the trawl is species-specific. The change in catch efficiency due to warp offset is likely minimal for species not captured as a function of herding and footrope escapement behaviors; however, because flatfish are susceptible to herding and are adept at footrope escapement, their catch rate could potentially be affected most by warp offsets.

Bridle efficiency (i.e., the fraction of fish in the area between the wing tips and doors that are herded into the path of the net) for flatfish catch is strongly influenced by the size of the herding area or area swept by the bridles because flatfish are stimulated to herd by the close approach or direct contact of the lower bridle. Although we were able to measure the off-bottom distance along the bridle and thereby predict the shape of the bridle, there is still considerable uncertainty as to the exact size of the herding area because the reaction height of a fish will vary with species, size, physiological state, state of arousal to the approaching bridle, viewing conditions for the fish, and, perhaps, other variables. Additionally, there is uncertainty in the estimate of the size of the herding area because it is based on the assumption of symmetry in the bridle angle-of-attack—a symmetry that is increasingly untenable with increasing offset. Despite this uncertainty, it is likely that the loss of herding area on one side of the trawl is not countered by an increase on the other side; thus some overall loss of herding efficiency is to be expected. In the hypothetical case chosen in our study, the reduction in herded area was 10.3%, which when applied to a strong herding flatfish such as rock sole (the herded component of the catch has been estimated to be about 49%, Somerton and Munro, 2001), the expected reduction in catch with an 8-m offset would be roughly 5%.

Flatfish escapement under the footrope will be influenced not only by the increase in off-bottom distance but also by the location along the footrope where the increase occurs. At a 7-m offset, the footrope off-bottom distance is about 2 cm higher in the footrope corner on the long side of the trawl and approximately 1 cm higher at the center and opposing corner than at zero offset (Fig. 12). Footrope off-bottom distances increased appreciably with greater offsets. Weinberg et al. (2002) demonstrated that flatfish escapement can increase with similar increases in footrope off-bottom distance; however their study focused on a different trawl and considered escapement for the entire footrope rather than by position along the footrope. Although we are unaware of any studies that quantify escapement rate by position along the footrope, our video observations indicate that flatfish are less likely to escape under the footrope near the wings than in the center (Somerton, unpubl. data). Because it is the center portion of the footrope where most of the increases in off-bottom distance occur in the 83-112 trawl, flatfish escapement is likely increased and potentially could represent a significant, but presently unquantifiable, loss in catch and a source of bias in estimates of relative abundance.

In conclusion, most aspects of the 83-112 Eastern trawl geometry were significantly degraded by warp offset differences equal to or greater than 7 m compared to zero offset. More importantly, the locations where the detectable differences occurred could affect catch efficiency; therefore a NOAA threshold value of 4% should be considered a maximum value for the 83-112 Eastern trawl and perhaps a more conservative value (less than 4%) would be prudent. However, given today's standardized survey procedures for measuring warp and for real-time monitoring of warp offset, the probability of warp offsets even approaching 7 m is highly unlikely on our surveys when locked-winches are used. Likewise, we argue that any appreciable differences in warp lengths between sides due to stretching are unrealistic because AFSC charter vessels use large diameter, compressed, solid-core wire. In fact, a review of the 413 hauls made during the 2004 EBS survey revealed that only three tows had a recorded maximum 1-m length difference between sides (Weinberg, unpubl. data).

Acknowledgments

We would like to thank Captain Brad Lougheed and the FV *Vesteraalen* crew, Niles Griffen, Waldemar Janezak, Van Ngo, and Todd Becker for their outstanding professionalism, positive attitudes, and constant attention to detail; AFSC scientists Stan Kotwicki and Dennis Benjamin for their assistance at sea; reviewers Guy Fleischer and Henry Milliken for their helpful comments; and the AFSC editorial staff, including Gary Duker, Jim Lee, and Karna McKinney for their help during the in-house review and manuscript preparation process.

Literature cited

Efron, B., and R. Tibshirani.
1993. An introduction to the bootstrap, 436 p. Chapman and Hall, New York, NY.

Fridman, A. L.
1969. Theory and design of commercial fishing gear. (Transl. from Russian by Israel Program Sci. Transl., Jerusalem) 1973, 489 p. [Available as TT 71-50129 from Natl. Tech. Inf. Serv., Springfield, VA.]

Munro, P. T., and D. A. Somerton.
2002. Estimating net efficiency of a survey trawl for flatfishes. Fish. Res. 55:267–279.

Somerton, D. A.
2004. Do Pacific cod (*Gadus macrocephalus*) and wall-

eye pollock (*Theragra chalcogramma*) lack a herding response to the doors, bridles and mudclouds of survey trawls? ICES J. Mar. Sci. 61:1186–1189.

2003. Bridle efficiency of a survey trawl for flatfish: measuring the length of the bridles in contact with the bottom. Fish. Res. 60:273–279.

Somerton, D. A., and P. T. Munro.

2001. Bridle efficiency of a survey trawl for flatfish. Fish. Bull. 99:641–652.

Somerton, D. A., and R. S. Otto.

1999. Net efficiency of a survey trawl for snow crab, *Chionoecetes opilio*, and Tanner crab, *C. bairdi*. Fish. Bull. 97:617–625.

Somerton, D. A., and K. L. Weinberg.

2001. The affect of speed through the water on footrope contact of a survey trawl. Fish. Res. 53:17–24.

Stauffer, G.

2004. NOAA protocols for groundfish bottom trawl surveys of the nation's fishery resources. NOAA. Tech. Memo. NMFS-F/SPO-65, 205 p. Alaska Fisheries Science Center, 7600 Sand Point Way N.E., Seattle, WA, 98115.

Venables, W. N., and B. D. Ripley.

1994. Modern applied statistics with S-plus, 462 p. Springer-Verlag, New York, NY.

Weinberg, K. L., D. A. Somerton, and P. T. Munro.

2002. The effect of trawl speed on the footrope capture efficiency of a survey trawl. Fish. Res. 58:303–313.

Weinberg, K. L., R. S. Otto, and D. A. Somerton.

2004. Capture probability of a survey trawl for red king crab (*Paralithodes camtschaticus*). Fish. Bull. 102:740–749.

Appendix 1: Estimating headrope and footrope shape when the warps differ in length

If a trawl headrope has the same shape as a flexible twine under a uniformly distributed load, then the shape of the headrope can be approximated as a quadratic (parabolic) function (Fridman, 1969; p. 84) as

$$y = cx^2, \tag{1}$$

where c is a constant controlling the shape (Fig. A1). As the headrope is distorted by a differential in warp length, not only does the value of c change, but the headrope is displaced along the path of the parabola, so that its center is no longer aligned with the vertex of the parabola. A unique solution to the shape of the headrope when it is distorted in this manner can be determined from three types of data: the total headrope length (L), the measured distance between the wing tips (W), and the measured slope (tangent) of the parabola at the center of the headrope (tan). The third quantity can be obtained from the V (perpendicular to the footrope) and U (tangential to the footrope) velocities measured by the headrope speed sensor as the quotient U/V. With these quantities, the solution can be obtained as follows.

A small length interval measured along the headrope can be expressed as

$$ds = (dy^2 + dx^2)^{\frac{1}{2}}. \tag{2}$$

Which, after substitution of the derivative of Equation 1, is

$$ds = \left(1 + (2cx)^2\right)^{\frac{1}{2}} dx. \tag{3}$$

The length of any segment of the headrope, measured from the port end (x_{lower}), is then

$$S = \int_{x_{lower}}^{x} \left(1 + (2cx)^2\right)^{\frac{1}{2}} ds. \tag{4}$$

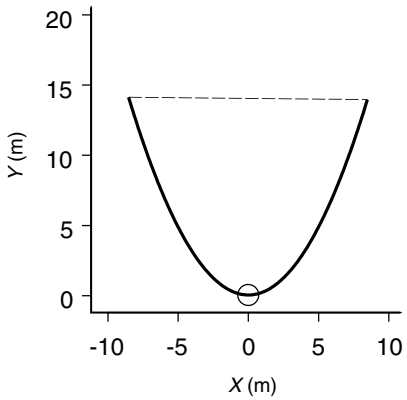

Figure A1

Shape of a trawl headrope as described by a parabola. The total length of the headrope (shown with a solid line) is equal to L. The measured width of the trawl (shown with a dashed line) is equal to W. The circle indicates the center of the headrope where a speed sensor is located. The speed sensor measures water speed both perpendicular and parallel to the headrope.

A segment equal to the total length of the headrope is obtained by integrating up to the starboard end (x_{upper}).

The solution is approximated numerically in two stages. First, for a trial value of c, Equation 4 is integrated from trial values of x_{lower} up to the value of x at which S=L/2 (i.e., x_{middle}). The tangent at this position is then evaluated as $2cx_{middle}$ (based on the derivative of Eq. 1). This process is then repeated iteratively to find the value of x_{lower} for the specified value of c at which the calculated tangent equals the tangent value determined from the headrope speed sensor. The value of x_{upper} is

then determined by integrating Equation 4 from x_{lower} to the value of x at which $S=L$. The wing tip to wing tip distance $D_{wingtip}$ is then calculated as

$$D_{wingtip} = \left((y_{upper} - y_{lower})^2 + (x_{upper} - x_{lower})^2\right)^{\frac{1}{2}}, \quad (5)$$

where y_{upper} and y_{lower} are obtained from Equation 1. In the second stage, c is varied and the above process is repeated iteratively until the value of $D_{wingtip}$ is found that is closest to the measured net spread. At this point the calculated values of $D_{wingtip}$ and the tangent at the headrope center will equal the measured values.

The headrope-shape model for each offset was used to project the off-bottom distances measured at the five positions along the footrope onto a plane orientated perpendicular to the direction of travel to depict the shape of the footrope as it would appear from a position in front of the trawl. To do this, a shape function was developed for the footrope. Assuming that the coordinates of the endpoints of the footrope (x_{lower}, x_{upper}, y_{lower}, y_{upper}) were the same as the headrope, Equation 5 was iteratively integrated with varying values of c until the estimated value of the footrope length (S) equaled the true length (34.1 m):

$$S = \int_{x_{lower}}^{x_{upper}} \left(1 + (2cx)^2\right)^{\frac{1}{2}} dx. \quad (6)$$

Once c is determined, Equation 4 is integrated to find the value of x associated with the value of S at each BCS (bottom current sensor) position on the footrope.